



# Experimental identification of structural changes and cracks in beams using a single accelerometer

Marcus Vinícius Manfrin de Oliveira Filho<sup>1</sup> · Juan Elías Perez Ipiña<sup>2</sup> · Carlos Alberto Bavastri<sup>1</sup>

Received: 6 June 2017 / Accepted: 1 November 2017 / Published online: 31 January 2018  
© The Brazilian Society of Mechanical Sciences and Engineering 2018

## Abstract

Several advances in the structural health monitoring field and in crack identification techniques were achieved in recent years. Nonetheless, the use of those techniques for crack identification in beams by the industry is still modest. A few reasons can be pointed to explain this fact: some proposed methods are unfeasible from the economic or logistic point of view, or the cracks are detected only when they already present an advanced depth, or the structures intended to be monitored are subjected to random loads, causing methods using deterministic excitations to be unrepresentative of the actual situation. Considering this, the objective of this study is to propose a method that could make it possible to identify and monitor cracks in beams aiming at operational conditions, i.e., a method to identify small cracks remotely and in almost real time, in beams subjected to unknown random loading, minimizing the measurement equipment used to a single accelerometer and a remote computer. To achieve so, the proposed method combines an operational modal analysis (OMA) based experimental procedure, a numerical-computational model of the damaged beam using the finite element method and an optimization problem, solved by using the genetic algorithm (GA). The method was preliminary tested on a steel beam, into which structural changes simulating cracks with different depths were inserted. The method was also tested on numerically generated data with noise. The found results are encouraging, since they have shown that crack position and depth can be determined with appropriate accuracy for many engineering applications. The limitations on the proposed method were also discussed.

**Keywords** Crack identification · Operational modal analysis (OMA) · Structural health monitoring (SHM) · Genetic algorithm (GA)

## 1 Introduction

In recent years, the increasing access to more accurate equipment, the possibility of remote data transmission in real time and the development of new physical and mathematical models have provided a significant improvement in the structural health monitoring (SHM) techniques.

Those techniques have straightforward applications in various branches of industry and engineering—such as mechanical, structural, civil, aeronautical and naval—for they guarantee an increased operational safety and decreased costs associated to maintenance. Beams are among the most studied elements in structural engineering due to their simplicity and wide range of applications. The identification and monitoring of damages that can appear in those elements is of particular interest since they allow an intervention in due time, thus avoiding the abrupt collapse thereof.

Several recent studies on the identification of cracks in beams have contributed to a better understanding of the physics of the problem, as well as the development of techniques and tools that allow a more precise and safer monitoring of this type of structure. However, from a technological point of view, one notices that the application of such technique by the industry is still modest and, in

---

Technical Editor: Kátia Lucchesi Cavalca Dedini.

✉ Marcus Vinícius Manfrin de Oliveira Filho  
marcus.oliveira.filho@gmail.com

Juan Elías Perez Ipiña  
juan.perezipina@fain.uncoma.edu.ar

<sup>1</sup> Federal University of Paraná, Rua Cel. Francisco H. dos Santos, s/n. 19011, Curitiba, PR 81531-980, Brazil

<sup>2</sup> CONICET, UNComa, Buenos Aires 1400, 8300 Neuquén, Argentina

some cases, even non-existing [1]. There is no single reason for this difficulty in adopting the techniques proposed by the academy, but a series of them, as discussed in the next paragraphs.

It is well known that the presence of cracks introduces local flexibilities in beams, by changing their dynamic and vibrational behavior [2]. By studying and monitoring those changes, it is possible to solve the so-called ‘inverse problem’, i.e., to determine which combination of crack position and depth produces the changes observed in those structural elements [3, 4]. The process of determining position and depth is usually called ‘identifying the crack’. The existing literature presents a variety of alternatives as possible solutions for different steps of the above-mentioned ‘inverse problem’. Among those steps, one can point out: the choice of dynamic and vibrational parameters to be monitored, the physical approach and the crack model used, peculiarities of the measuring system used (if any), and the optimization algorithm used.

The vibrational parameters usually monitored aiming at identifying cracks are the natural frequencies, the vibration modes and the frequency response function (FRF) of intact and damaged beams. Given their relative measurement facilities, there is also the possibility of controlling two of those parameters simultaneously. Several studies [5–13] solved the inverse problem by controlling changes that cracks provoke on the beam’s natural frequencies. In their works, Nikolakopoulos et al. [4] and Owolabi et al. [14] presented three-dimensional graphs relating the position and depth of cracks to the percentage reduction they produced on the natural frequencies of beams. When the percentage reduction on a natural frequency is known, it is possible to extract a curve from those three-dimensional graphs, which contain all possible combinations of positions and depths of cracks that produce this specific change [11]. When the reduction of three different natural frequencies is known, it is possible to superimpose their curves. It was observed that the curves intercept each other on a single point, which provides the single combination of position and depth of crack that produces the known decrease pattern on the natural frequencies. Owolabi et al. [14] also showed that the minimum number of natural frequencies monitored to identify cracks must be equal to the number of searched parameters plus one. Thus, when one wishes to identify a single crack (to determine its depth and position), one must monitor the reduction pattern of three natural frequencies. When the identification of two cracks is desired (two depths and two positions), the monitoring must be performed on five natural frequencies, and so on so forth. Later, Greco and Pau [15] drew similar conclusions, also pointing out that the minimum number of controlled natural frequencies may not be enough to guarantee the precise solution of the inverse problem in the

presence of experimental errors. Instead of studying the natural frequencies, some researchers tried to solve the inverse problem by monitoring the vibration modes of damaged beams [1, 3, 16–20]. Other researchers have studied the effects of cracks on natural frequencies and vibration modes simultaneously [21–25]. Finally, the works by Owolabi et al. [14] and Saeed et al. [26] studied the effects of cracks in beams on natural frequencies and their FRF’s.

Beside the parameters to be monitored, the literature also reports different possibilities of physical models to be used in solving the inverse problem of identifying cracks in beams. Some studies used the Euler–Bernoulli beam model [9, 11, 15, 22, 27]. Other researchers used more sophisticated beam models, which took into account also the effects produced by shear strain [12, 28–30]. Some studies have modeled cracks in beams as torsional springs [6, 9, 11], others as associations of torsional and translational springs [21, 28, 30]. Other alternative approaches for the physical modeling of the problem can also be found in the works of Law and Lu [31], Andreaus and Baragatti [32] and Neves et al. [33]. Bovsunovsky and Surace [34] wrote a review article on non-linearity in vibrations of elastic structures with closing cracks.

From the mathematical point of view, different methods and algorithms have already been used to solve the inverse problem in identifying cracks. Aiming at amplifying details about the vibration responses of damaged beams, some studies laid hands on techniques based on the Wavelet Transform (WT) [1, 16, 20, 21]. Nikolakopoulos et al. [4] and Owolabi et al. [14] proposed graphic methods to identify cracks in beams. Depending on the approach, the inverse problem can lead to an optimization problem: some researchers applied the Newton–Raphson method to solve it [3, 6], whereas others based their work on the use of genetic algorithms (GA) [12, 23, 29]. Alternatively, Saeed et al. [26] and Hakim et al. [24] used the artificial intelligence (artificial neural networks—ANN) and Moezi et al. [9] used the Cuckoo optimization algorithm. It is worth pointing out that not only the optimization technique used to solve the inverse problem differed in above-mentioned researches. In addition, the optimization problem modeling also differed in all of these studies, i.e., different objective functions and restrictions aiming at identifying cracks in beams were proposed.

Finally, there are also different possibilities for acquiring the vibrational experimental data used in the inverse problem. Some researchers extracted data using the experimental modal analysis (EMA) [3, 11, 12, 14, 24], whereas Xu et al. [20] used an operational modal analysis (OMA). The basic difference between the two methods is that, in the EMA, the input function (excitation force) is a known function, whereas, in the OMA, it is unknown—

frequently, the excitation in the OMA occurs during the natural operation of the structure. Although the EMA provides more accurate results, it demands a specialist to test the structure, normally with a piezoelectric hammer or with a shaker, which can be prohibitive in terms of a SHM technique [35].

This large array of possibilities present in the steps that make up a problem of identifying cracks in beams turns out to be a difficulty found in adopting a SHM technique, since it raises questions and doubts regarding different peculiarities, advantages and disadvantages of each application.

Beside these different possibilities, a frequent subject discussed in the literature is the difficulty on identifying cracks in incipient stages. It is known that the shift pattern that cracks provoke on natural frequencies and mode shapes depends on damage localization, while the amplitude of these shifts depends on damage severity. In other words, hypothetical cracks located in the same position would cause the same changes on the beam's vibrational parameters, but deeper cracks would make these effects more evident [8, 14, 36–38]. The changes on a beam's dynamic behavior caused by small cracks ( $a/h < 10\%$ , where  $a$  is the crack's depth and  $h$  is the beam's height) may be of the same order of magnitude of errors associated with the numerical models and the equipment utilized to solve the inverse problem. Therefore, this type of crack is difficult, or even impossible, to be identified.

This subject was earlier discussed by Douka et al. [16], which pointed out the difficulty in identifying cracks with a proportion  $a/h < 20\%$ . In some studies, cracks introduced in numerical models of beams were identified, as follows: Lee [39] identified cracks with a relative depth of  $a/h = 20\%$ ; Saeed et al. [26] identified cracks with a relative depth of  $a/h = 16.7\%$  in curved beams; Lee [6], Attar [22] and Khiem and Tran [19] identified cracks with a depth of  $a/h = 10\%$ . The problem becomes even more complex when cracks are desired to be identified experimentally, because, in these cases, the acquired data is always susceptible to experimental errors. Cracks in beams with the following relative depths were identified experimentally in earlier studies:  $a/h = 50\%$  [11];  $a/h = 33\%$  [8];  $a/h = 30\%$  [17];  $a/h = 25\%$  [40];  $a/h = 20\%$  [9, 23];  $a/h = 16.7\%$  [21];  $a/h = 15\%$  [12, 41];  $a/h = 11\%$  [13];  $a/h = 10\%$  [42]. In a recent study, He and Ng [43] observed the effect of multiple cracks in beams. A crack having a depth of  $a/h = 33\%$  was identified with an error of 43.51%. Observing these studies, one can see that, to the best of our knowledge, the smallest identified cracks in beams—numerically or experimentally—have a depth of  $a/h = 10\%$ . However, from the fracture mechanics and predictive maintenance point of view, this depth might be considered already too advanced, arising unacceptable risks for the operational safety depending on the

application. Therefore, there is an obvious industrial interest in detecting damages in beams in less advanced stages.

Based on the considerations presented in the previous paragraphs, the four main issues that bring difficulties for the industry to adopt the techniques proposed by the academy can be synthesized as follows: (1) there is a large array of possibilities in each of the steps of the crack identification problems, which causes several doubts and questions; (2) some proposed methods require the use of a set of expensive equipment and qualified labor force for in situ inspections in order to obtain vibrational data, which turns the application of that technology unfeasible from the economic or logistic point of view; (3) some technologies only manage to detect cracks when they already present an advanced depth (more than 10% of the beam's height), which can bring about unacceptable structural risks; (4) beams may be subject to random loads, which introduce more complexities into the load characterization problem and may cause methods using deterministic excitations become unrepresentative of the actual situation.

Considering this context, the objective of this study is to step forward in the direction of turning the previous studies achievements and techniques more applicable, by proposing a method that makes it possible to identify and monitor cracks in beams in almost real time in a semi-automatic way, without the need of local inspection to acquire vibrational data. The proposed method aims at the SHM in operational conditions, i.e., to be able to detect the damage in a relative initial stage (cracks with depths smaller than 10% of beam's height), in structures subject to random loading and minimizing the quantity of hardware utilized to acquire data to a notebook (remote) and a unique sensor installed on the beam. The proposed method was preliminary tested on a steel beam with a square cross-section into which a cut simulating a crack was introduced. The depth of the cut was gradually increased and, finally, a second cut was introduced into the beam. Besides this experimental evaluation, the effectiveness of the methodology was also tested on numerically generated noisy data. The results are presented in Sect. 4. The limits in its application of the method were also discussed.

## 2 The proposed method

From data acquiring to its treatment, all the necessary steps and decisions for the implementation of the proposed method were developed and taken aiming at its use in an operational way. Some studies can illustrate the importance of the use of an appropriate monitoring system for SHM applications [38, 44–46]. In order to reduce the measurement system used, the option adopted was to control the

natural frequencies of the beam, considering that a single accelerometer suffices to acquire data about that parameter. Besides, natural frequencies are easier to measure and less susceptible to measurement errors than vibration modes [10]. In order to obtain this parameter experimentally, it was also decided to perform an OMA based data acquiring of the beam. The drawback concerning the EMA is that it requires the work of specialists in situ, which would make it impossible to monitor the damage in real time, in addition to being unfeasible when the structures are numerous or located in hard-to-reach places. For simplicity reasons, a shaker was used to provoke the excitation on the beam. However, the equipment was disconnected from the software, which means the excitation force acting on the structure was unknown, characterizing the OMA. In real applications, this step could be substituted by the natural application of the beam, with the excitation being provided by the movement of a machine or wind forces, for example.

A comment becomes pertinent at this point: although the term ‘natural frequency’ is used indiscriminately in many scientific articles, very often the natural frequency is associated to a mechanical system without damping; when an OMA is performed to acquire vibrational data (acceleration response model in frequency), the peak frequencies observed are slightly different from the natural frequencies. Thus, in the present work, those peak frequencies are referred to as ‘resonant frequencies’, and the term ‘characteristic frequencies’ is used indistinctly for referring to both the natural and the resonant frequencies. It is possible, however, to use the resonant frequencies data obtained experimentally to make comparisons with natural frequency data generated numerically, provided one adopts the premises and hypotheses presented in Sect. 2.2.

A two-dimensional numerical-computational model based on the finite-element method and an optimization problem solved by using GA were proposed, aiming at giving speed and reliability to the solution of the inverse problem, since a considerable number of simulations is necessary. Although recommendations were taken from the literature for solving de optimization problem using the GA, a new objective function based on the variations of the first five natural frequencies of the beams was proposed. The three steps necessary for the implementation of the presented method can be summarized as below:

- An OMA based measurement of the beam to obtain the resonant frequencies before and after damage. With those values, the decrease pattern is plotted on the values of the characteristic frequencies. It is important to notice that, when an accelerometer is installed on a supposed intact beam, it will automatically acquire data referring to the “before damage” state. If this data is acquired periodically, one should expect changes on the

resonant frequencies values if cracks appear and, if the values remain the same, it shall indicate that the beam remains in an undamaged state;

- A numerical-computational model—created by using the finite-element method—capable of simulating the effect of cracks in different positions and depths. This computational model of the structure should be prepared before the application of the method. The same model could be used in order to monitor the integrity of similar structures as, for example, components of several machines of the same model (although the experimental data acquired from each one of them would be slightly different, due to small constructive differences);
- An optimization problem, the objective function of which aims at decreasing error between the changing pattern obtained experimentally and numerically. When such difference is small enough, the optimization algorithm will have identified the crack, i.e., it will have determined, with acceptable accuracy, its depth and location;

Each of these parts is presented in detail bellow. The experimental procedure and the numerical-computational model are explained first, defining the parameters obtained in each of these steps. Later, the proposed optimization problem is presented, pointing how experimental and numerical data are utilized. The method presented was applied to a SAE 1020 steel beam, with an elastic modulus  $E = 205$  GPa and density  $\rho = 7860$  kg/m<sup>3</sup>. The beam was 720 mm long with a square cross-section (22.23 mm of width and height).

## 2.1 Experimental procedure

The experimental procedure is based in an OMA, aiming at identifying the resonant frequencies of the beam, first in the intact condition and then in the presence of damages. It is worth pointing out that the term OMA is normally used to refer to an experimental procedure that obtains the modal parameters of a structure; however, using a single accelerometer, it is not possible to determine the structure’s mode shapes, but only the resonant frequencies. The first step of the proposed method is to determine the number of characteristic frequencies to be monitored. It is worth pointing out that, from the experimental point of view, as the characteristic frequencies assume higher values, the difficulty in experimental acquisition also increases for it is necessary to have an equipment with a higher data processing capacity. As there is the intension of identifying two cracks in the tested beam, a monitoring of its first five natural frequencies was carried out, as discussed earlier.

At the experimental stage, a single uniaxial accelerometer, used to capture frequency acceleration response, was placed at  $x_a/L = 0.02$ , where  $x_a$  is the accelerometer position and  $L$  is the length of the beam. In order to excite the structure, a shaker was used, placed at  $x_s/L = 0.39$ , where  $x_s$  is the position of the shaker. These accelerometer and shaker locations were chosen taking special care not to position them on the node of any of the first five vibration modes of the structure, which would cause information on the corresponding natural frequency to be lost. The beam was tested in a free–free boundary condition, and the shaker was configured to produce a random excitation on the beam (white noise). It is emphasized that the excitation function of the shaker was not used to determine the response of the structure—the OMA uses just the response data. Figure 1 illustrates the measurement scheme used.

The accelerometer PCB Piezotronics® (model 352C68) was connected to an acquisition card of a computer. First of all, beam data in intact condition were obtained. This is a crucial step for the level of detail one is searching for: tests were performed in testing bodies in the intact condition, but the small differences found in theoretically identical bodies (about 0.1% of variation on the resonant frequencies values) are already of the same order of magnitude of the

changes produced by cracks with small depths—see Table 3 for more results. This effect could impair the application of the proposed method, because a false crack could be identified. It is therefore pointed out that the beam to be used must be primarily assessed, i.e., its acceleration response curve in frequency must be measured.

Later, using a thin saw, cuts with 0.5 mm width were introduced simulating open cracks in the beam. Since cuts are not real cracks, the term “crack” was avoided in the present text when referring to this experimental procedure. Instead, the terms “structural change” or “cut” were preferably used. At each cut increase, a new measurement was performed under the same conditions. Finally, after the structural change reached a depth of  $a/h = 50\%$ , a second cut was introduced to the same beam, and a double damage (referred here as “double crack”) case was also studied, as further discussed. Regardless of this terminology precaution, the procedure of using saw or electrode cuts in order to simulate cracks is well reported in the literature [3, 8, 11, 14, 21, 31, 47, 48]. Using the acceleration response curves in frequency, five peak frequencies of the beam (here referred to as ‘resonant frequencies’) were determined.

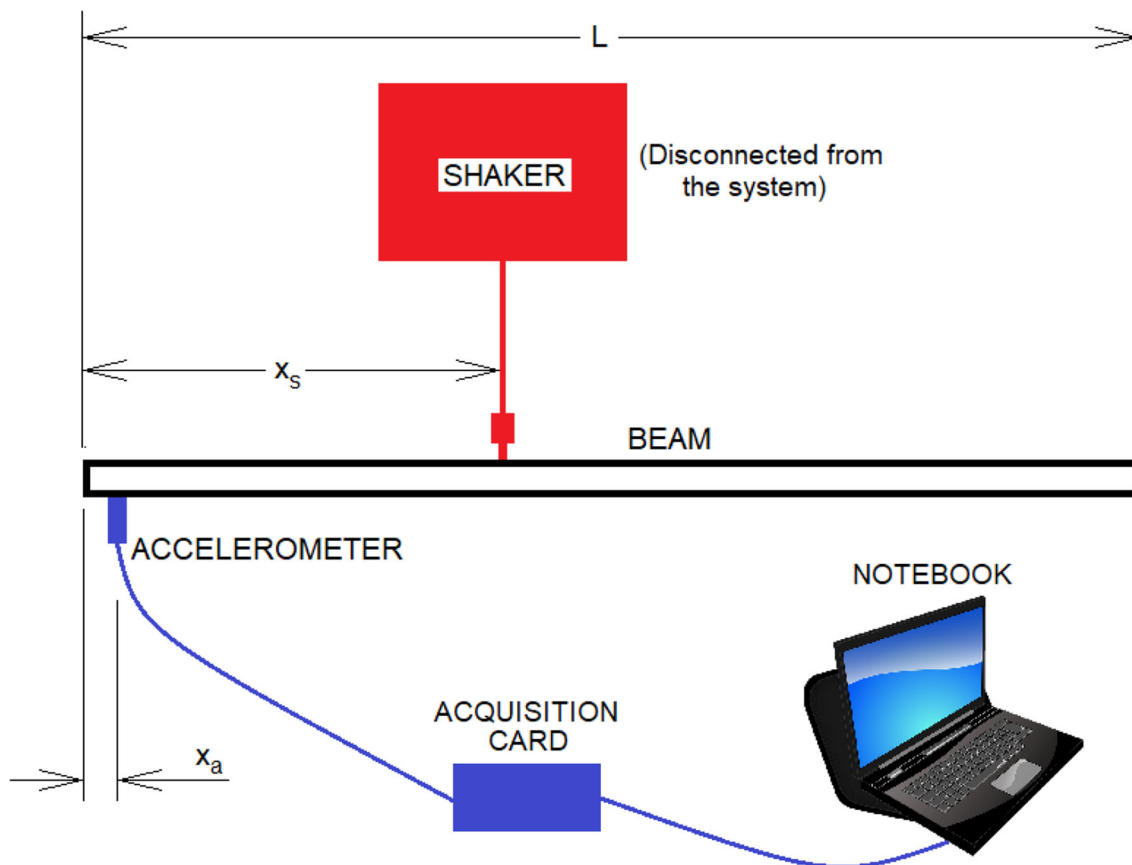


Fig. 1 Measuring system adopted

The data acquisition software installed in the computer was the RT Pro Photon v. 6.3307. This software allowed the user to set the frequency band in which the measurement would be performed (always starting at 0 Hz) and the number of points to be acquired in the frequency domain, up to a maximum of 1800 points. Therefore, narrow frequency bands allow a better data resolution, since the increment in frequency is smaller. In order to obtain the best possible resolution for each of the resonant frequencies analyzed, each measurement was performed in three different frequency bands. The three measured bands were: from 0 to 300.00 Hz (increase of 0.16667 Hz); from 0 to 1318.26 Hz (increase of 0.73242 Hz); from 0 to 4500 Hz (increase of 2.5 Hz). This way, it was possible to obtain more accurate data about the first resonant frequency of the beam (located in the first measuring band), data with an intermediate accuracy on the second and third resonant frequencies (between 300.00 and 1318.26 Hz) and less accurate data regarding the fourth and fifth resonant frequencies (between 1318.6 and 4500 Hz). A Hanning window was used to acquire the structure acceleration response data.

With the purpose of illustrating the performed measurements, Fig. 2 presents the acceleration response graph in the frequency domain, obtained for the beam both in intact condition and with an  $a/h = 50\%$  deep structural change, where  $a$  is the depth of the damage and  $h$  is the

height of the beam. In the graph it is possible to observe the first five resonant frequencies of the beam in both measurements—the first five resonant frequencies of the beam in the intact condition  $fe_i^I$  are highlighted (see Table 1 for the exact measured values).

Analyzing the graph, one can see that the resonant frequencies decreased in the presence of the structural change. The percentage change produced by the structural change or crack on the  $i$ th resonant frequency obtained experimentally is given by:

$$ED_i = 100 \left( 1 - \frac{fe_i^C}{fe_i^I} \right), \quad (1)$$

where ED is the experimental difference of the resonant frequency of the experimental data,  $fe^C$  is the resonant frequency of the cracked beam, and  $fe^I$  is the resonant frequency of the intact beam, obtained experimentally. As the resonant frequency of the damaged beam,  $fe^C$ , is always lower than the natural frequency of the intact beam,  $fe^I$ , ED always assumes a positive value.

### 2.1.1 Simulated data

Besides the data obtained experimentally, an intact beam case and five different damage scenarios were also simulated numerically, allowing the testing of the method

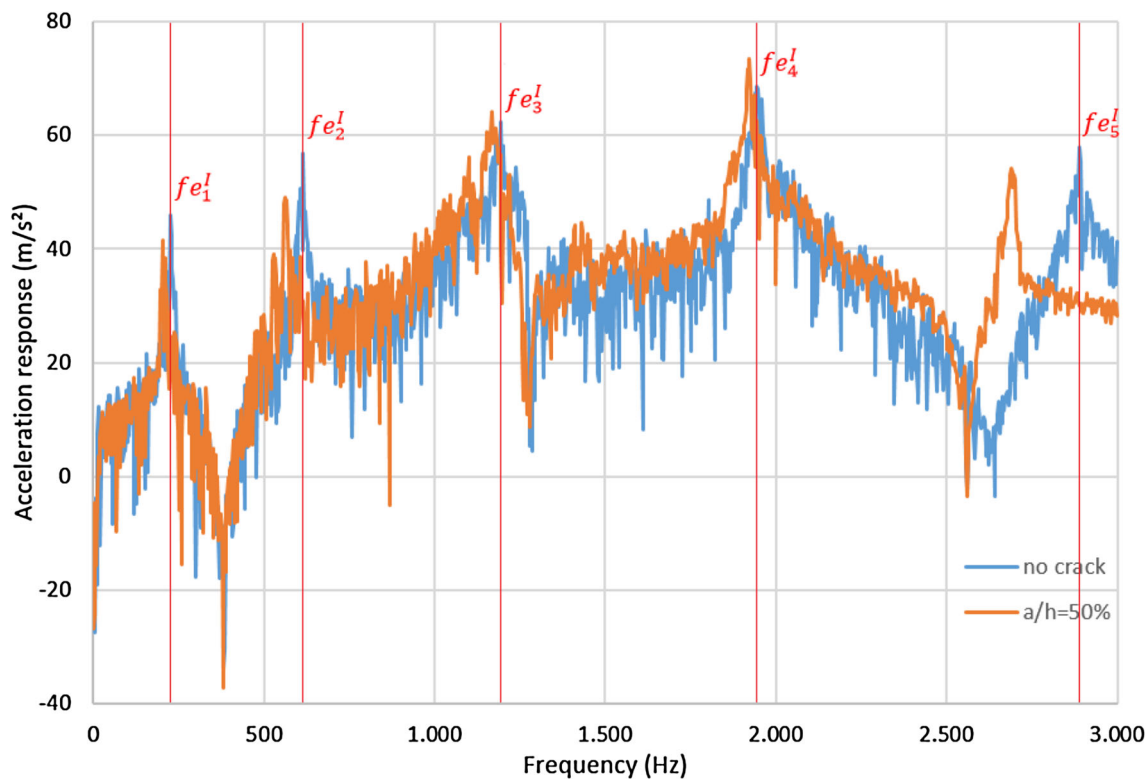


Fig. 2 Acceleration response in the frequency domain for intact and cracked beams

**Table 1** Comparison between resonant frequencies of the beam for each case (experimental data)

| No crack   | $fe_1^l$ (Hz) | $fe_2^l$ (Hz) | $fe_3^l$ (Hz) | $fe_4^l$ (Hz) | $fe_5^l$ (Hz) |
|--|---------------|---------------|---------------|---------------|---------------|
|  | 224.1667      | 614.5020      | 1193.8477     | 1945.0        | 2890.0        |
|  | $fe_1^c$ (Hz) | $fe_2^c$ (Hz) | $fe_3^c$ (Hz) | $fe_4^c$ (Hz) | $fe_5^c$ (Hz) |
| Case 1: $a/h = 5\%$<br>$a = 1.1$ mm<br>$x_c = 22.0$ cm   | 224.0000      | 613.7695      | 1193.8477     | 1945.0        | 2887.5        |
| Case 2: $a/h = 10\%$<br>$a = 2.2$ mm<br>$x_c = 22.0$ cm  | 223.6667      | 612.3047      | 1192.3828     | 1945.0        | 2882.5        |
| Case 3: $a/h = 20\%$<br>$a = 4.4$ mm<br>$x_c = 22.0$ cm  | 222.5000      | 606.4453      | 1189.4531     | 1942.5        | 2860.0        |
| Case 4: $a/h = 50\%$<br>$a = 11.1$ mm<br>$x_c = 22.0$ cm   | 210.5         | 560.3027      | 1166.7480     | 1922.5        | 2690.0        |
| Case 5 (double crack): $a_1/h = 50\%$<br>$a_2/h = 25\%$<br>$a_1 = 11.1$ mm<br>$x_{c1} = 22.0$ cm<br>$a_2 = 5.5$ mm<br>$x_{c2} = 59.0$ cm | 209.6667      | 553.7109      | 1141.1133     | 1890.0        | 2662.5        |

effectiveness in more situations. In order to obtain these numerical results, a parameterized computational model of a free–free beam was created numerically through the finite-element method using the commercial software ANSYS, as described in more details in Sect. 2.2. The beam was excited by a unitary harmonic force and the acceleration response in the frequency domain (inertance) was evaluated in the range of 0–3000 Hz with increments of 0.16667 Hz, which was the best resolution allowed by the accelerometer in the experimental setup.

The exciting force was applied in the coordinate  $x_s/L = 0.39$  and the response was analyzed in  $x_a/L = 0.02$ , which were the same positions of the shaker and the accelerometer in the experimental procedure, respectively. Normally distributed noise (white noise) was added to the inertance functions obtained numerically, with the objective of turning these computationally generated responses closer to experimental data. The standard deviation of the white noise was estimated to simulate effects that are consistent to experimental error (see Fig. 2). The Fig. 3 illustrates the response obtained for a beam with a known crack, before and after the addition of the noise.

The five different damage scenarios are presented in Table 2 (Cases 6–10). As in the experimental setup, the peak frequencies of the graphs were observed and the percentage differences produced by the cracks were calculated according to the Eq. (1). With the objective of facilitating the understanding, both the data obtained experimentally and this numerically generated data with

noise are referred as “experimental data” or “obtained experimentally”.

## 2.2 Computational model

Using the ANSYS software interface, and considering that only the characteristic frequencies associated to the bending in the axis of crack opening and closing were obtained experimentally by the uniaxial accelerometer, one opted to use a two-dimensional model of the beam (longitudinal section), which leads to the same results of a three-dimensional model in the studied axis, at a lower computational cost. Plane isoparametric elements with 8 nodes were selected and the mesh was refined until it provided sufficient accuracy, of the same order of magnitude of those differences observed over the resonant frequencies in the OMA data. The elements had an average side size of 0.72 mm, resulting in a mesh formed by about 16,560 elements (this number has small variations according to the simulated crack position and depth). Each iteration took about 20 s to be performed, using an i5 quad-core with 4-gigabyte RAM computer. In average, it took about 1 h and 30 min for the optimization problem to be solved, i.e., for the crack to be identified (the time increased to a few hours in the double crack identification problem), but it was verified that this time could be shorter if a more powerful computer was used.

A free–free boundary condition was set in the numerical model, in order to make a direct comparison with the

**Fig. 3** Inertance response obtained for a beam with a crack (before and after noise conditions)

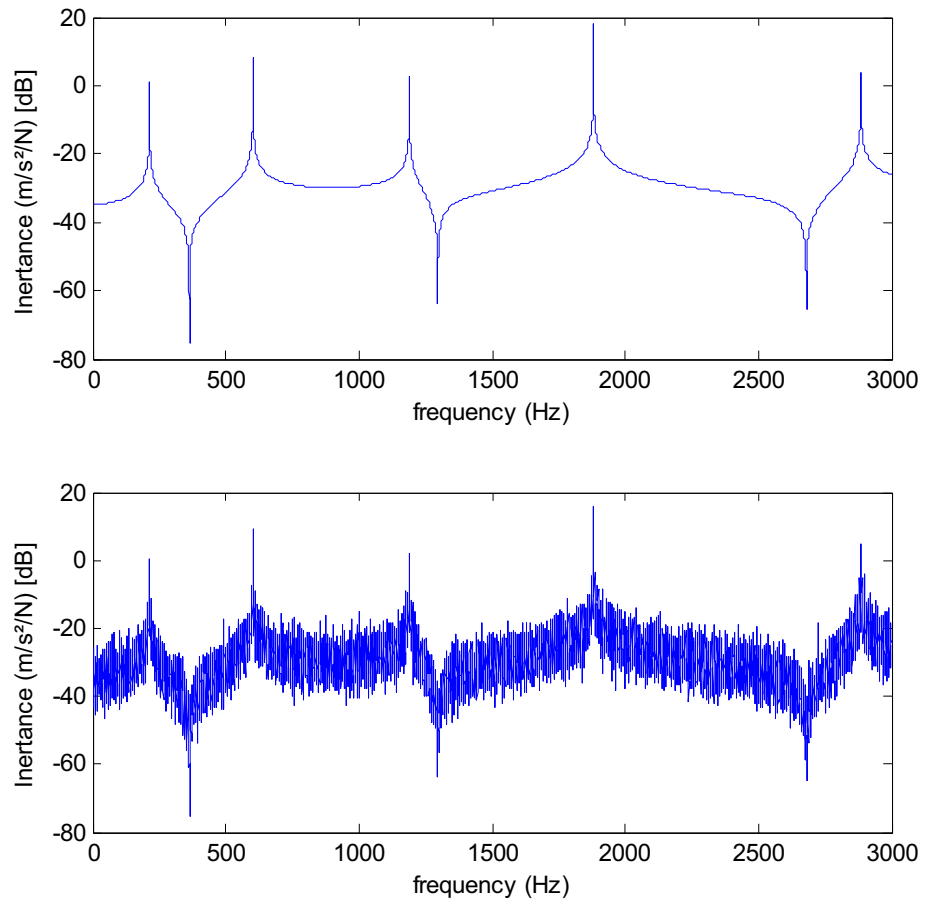


**Table 2** Comparison between resonant frequencies of the beam for each case (numerically generated noisy data)

| No crack   | $fe_1^l$ (Hz) | $fe_2^l$ (Hz) | $fe_3^l$ (Hz) | $fe_4^l$ (Hz) | $fe_5^l$ (Hz) |
|--|---------------|---------------|---------------|---------------|---------------|
|  | 225.5         | 617.3333      | 1200.3333     | 1961.1667     | 2889.0        |
|  | $fe_1^c$ (Hz) | $fe_2^c$ (Hz) | $fe_3^c$ (Hz) | $fe_4^c$ (Hz) | $fe_5^c$ (Hz) |
| Case 6: $a/h = 8\%$<br>$a = 1.77$ mm<br>$x_c = 12.0$ cm  | 225.6667      | 617.1667      | 1198.0        | 1957.0        | 2884.6667     |
| Case 7: $a/h = 15\%$<br>$a = 3.32$ mm<br>$x_c = 50.8$ cm   | 224.6667      | 613.5         | 1197.1667     | 1960.6667     | 2875.1667     |
| Case 8: $a/h = 23\%$<br>$a = 5.10$ mm<br>$x_c = 31.0$ cm   | 221.6667      | 615.3333      | 1191.8333     | 1943.3333     | 2883.8333     |
| Case 9: $a/h = 40\%$<br>$a = 8.86$ mm<br>$x_c = 43.2$ cm   | 213.5         | 602.5         | 1189.1667     | 1881.1667     | 2885.0        |
| Case 5 (double crack):<br>$a_1/h = 30\%$<br>$a_2/h = 18\%$<br>$a_1 = 6.65$ mm<br>$x_{c1} = 27.0$ cm<br>$a_2 = 3.99$ mm<br>$x_{c2} = 63.0$ cm | 220.0         | 605.5         | 1193.8333     | 1903.6667     | 2840.1667     |



experimental data. It is important to notice that a modal analysis was performed at this stage, which is different from the harmonic analysis described in Sect. 2.1.1. Besides the natural frequencies, the mode shapes are also calculated in the analysis. Although it can be seen that they are directly affected by the presence of cracks, this information was not used, since no data regarding the mode shapes were obtained experimentally.

Figure 4 illustrates the 2D numerical-computational model of the beam with a crack.

The equation of motion of the system in Fig. 4 with multiple degrees of freedom is given by [49]:

$$[m]\ddot{x} + [c]\dot{x} + [k]x = f, \tag{2}$$

where  $[m]$ ,  $[c]$  and  $[k]$  are the mass, damping and stiffness matrices, respectively;  $x$  is displacement,  $\dot{x}$  is speed,  $\ddot{x}$  is acceleration and  $f$  is the external effort of the system. From this equation, one obtains an eigenvalue problem, solved in the calculation routine of the ANSYS software in order to obtain the natural frequencies of the numerical model. If the system is undamped,  $[c] = 0$ , and the generalized eigenvalue problem is given by:

$$\lambda_i[m]\phi_i = [k]\phi_i, \tag{3}$$

where  $\lambda_i$  is the  $i$ th eigenvalue,  $\phi_i$  is the corresponding  $i$ th eigenvector and the natural frequencies  $f_{n_i}$  are given by  $f_{n_i} = \sqrt{\lambda_i}$ . For a one-degree-of-freedom damped system, the natural frequency and the resonant frequency for the acceleration response model in frequency (inertance) are given by, respectively:

$$f_n = \sqrt{\frac{k}{m}}, \tag{4}$$

$$f_r = \frac{f_n}{\sqrt{(1 - 2\xi^2)}}, \tag{5}$$

where  $f_n$  is the natural frequency,  $f_r$  is the resonance frequency,  $k$  is stiffness,  $m$  is mass, and  $\xi$  is the damping factor of the system. Considering—without losing generality—the appearance of an external effect such as a crack,

which produces a change in the system stiffness, maintaining mass and damping practically constant, it is possible to estimate the percentage difference between those resonant frequencies due to that change, the following way:

$$D_r = 100 \left( 1 - \frac{f_{r1}}{f_{r2}} \right) = 100 \left( 1 - \frac{\sqrt{\frac{k_1/m}{(1-2\xi^2)}}}{\sqrt{\frac{k_2/m}{(1-2\xi^2)}}} \right) = 100 \left( 1 - \sqrt{\frac{k_1}{k_2}} \right), \tag{6}$$

where  $D_r$  is the difference (%) of the resonant frequencies of a damped system,  $k_1$  is stiffness of the system in state 1 (before the change) and  $k_2$  is the stiffness of the system in state 2 (after the change).

If a change is produced in a way to change the stiffness of a one-degree-of-freedom system without damping, while maintaining the mass constant, it is possible to estimate the percentage difference between natural frequencies before and after the change as follows:

$$D_n = 100 \left( 1 - \frac{f_{n1}}{f_{n2}} \right) = 100 \left( 1 - \frac{\sqrt{\frac{k_1}{m}}}{\sqrt{\frac{k_2}{m}}} \right) = 100 \left( 1 - \sqrt{\frac{k_1}{k_2}} \right), \tag{7}$$

where  $D_n$  is the difference (%) of natural frequencies of an undamped system. According to Eqs. (6) and (7), one notices that the percentage difference produced by a change only in the stiffness on the characteristic frequencies (natural and resonant) does not depend on the system being damped or undamped, i.e.,  $D_r = D_n$ .

The reasoning presented for a one-degree-of-freedom system may be extrapolated to a multiple-degree-of-freedom system, as is the case of the beam under study. Then, the hypothesis of the present work is that the crack produces changes only in the stiffness matrix of the system, and that the mass and damping matrices remain invariant when cracks are produced. This hypothesis can be justified

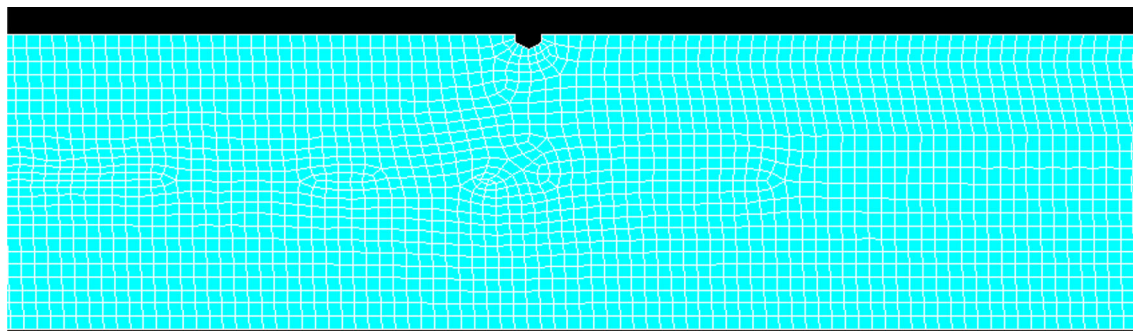


Fig. 4 Numerical-computational model

by the following causes: the mass loss of the beam caused by a crack is negligible when compared to the total mass of the beam; small cracks provoke negligible effects over system's damping; open cracks, as in the case of the present study, reduce the friction between the two crack contact areas, thus reducing the energy loss and keeping the damping of the system practically constant.

Because of this effect—percentage differences on the resonant frequencies obtained for a viscous damped system is equal to those percentage differences obtained for the natural frequencies of an undamped system—it was possible to consider the system as undamped in the numerical model used. Such choice is especially convenient since it avoids the need for estimating the structure damping, besides speeding up calculations during the optimization problem, described in Sect. 2.3.

### 2.2.1 Numerical model

First, a simulation of the intact beam was performed, in order to obtain the numerical natural frequencies of the undamaged structure. Next, cracks modeled in the shape of a pentagon—an association of a rectangle and an isosceles triangle—were introduced, with a constant width value parameterized according to beam's length (0.5 mm in this study). Although this geometry was chosen aiming at giving some realism to the simulation, the results of the work carried out by Orhan et al. [48] have shown that the natural frequencies estimated in numerical models are insensitive to different geometrical shapes of cracks. The damage was inserted into the model by varying parameters  $x_c$  and  $a$ —position and depth of crack, respectively—and the natural frequencies were recalculated. The changes produced by the crack in the  $i$ th natural frequency of the numerical model is given by:

$$ND_i = 100 \left( 1 - \frac{fn_i^C}{fn_i^I} \right), \quad (8)$$

where ND is the numerical difference (%) of the numerical model natural frequency,  $fn^C$  is the natural frequency of the cracked beam of the numerical model, and  $fn^I$  is the natural frequency of the intact beam of the numerical model. As the natural frequency of the damaged beam,  $fn^C$ , is always lower than the natural frequency of the intact beam,  $fn^I$ , ND always assumes a positive value.

## 2.3 Optimization problem

Starting from the accepted hypotheses and knowing the percentage differences that structural changes and cracks produce on the experimental data and on the numerical model— $ED_i$  and  $ND_i$ , respectively, an optimization

problem was proposed aiming at identifying these damages. As the reduction pattern of natural frequencies generated by a crack is unique, depending its position and depth, the present work adapts the idea proposed by Owolabi et al. [14] for identifying the structural change in a graphic way into an optimization problem, eliminating the problem of errors arisen due to linear interpolations and giving speed to the solution. The proposed optimization aims at approximating the changing pattern produced by cracks in the numerical-computational model to the pattern obtained experimentally, i.e., to minimize the difference between them. Thus, the objective function  $S$  to be minimized was defined, as given by:

$$S(x) = \sum_{i=1}^N (ED_i - ND_i)^2, \quad (9)$$

where  $N$  is the number of characteristic frequencies used to identify the damages and  $x$  is the project vector given by  $a$  and  $x_c$ . Restrictions were imposed to the parameters searched in the problem (position  $x_c$  and depth  $a$  of the crack), as follows:

$$0 \leq x_c \leq L, \quad (10)$$

$$0 \leq a \leq 0.9h. \quad (11)$$

When the optimization problem is solved aiming at identifying two cracks, four restrictions must be imposed:

$$0 \leq x_{c1} \leq L, \quad (12)$$

$$0 \leq x_{c2} \leq L, \quad (13)$$

$$0 \leq a_1 \leq 0.9h, \quad (14)$$

$$0 \leq a_2 \leq 0.9h, \quad (15)$$

where  $x_{c1}$ ,  $x_{c2}$ ,  $a_1$  and  $a_2$  are the position and depth of cracks 1 and 2, respectively.

The inverse problem was solved by using genetic algorithms (GA) as the optimization method. The GA is a method based on the natural evolution from Darwin's theory. Basically, an initial population is defined randomly, with possible candidates for solving the problem. In the present case, a candidate is composed by two variables: crack's depth and position. After this first generation is tested, the best-fitted candidates are kept for the next generation—sometimes called the “elite count” or “champions”, while the rest of the generation suffers from mutation and crossover. The process goes on until a virtually best individual is found, i.e., a combination of crack's depth and position that agrees the most with experimental data.

The choice of that method is convenient, since it does not need an initial candidate—initial depth and position of the crack—to start solving the optimization problem. The definition of an initial candidate is an obstacle in this

process of optimization, since the solution may converge to a local minimum, leading to a false position and depth of the crack. On the contrary, the initial population of the GA is distributed throughout the search space, which increases the probability of determining the global minimum of the function. A pertinent comment is that preliminary tests were conducted using the Nelder-Mead method for solving the optimization problem, which demands the choice of an initial candidate. Although this method had an advantage regarding the simulation time (the Nelder-Mead method took about 75% of the necessary time for the optimization to be solved by the GA), the optimization converged to a local minimum in approximately half of the attempts, leading to false crack positions and depths, which is not admissible in terms of a SHM technique. Using the GA, 100% of the cracks were identified correctly, as shown in the results. Besides, the use of the GA for solving this kind of problem is already established in the literature [11, 29].

The initial population was selected consisting of 15 times the number of variables. When optimization was performed aiming at identifying a single damage, two parameters were being searched ( $x_c$  and  $a$ ), and the initial population was defined as 30. When optimization was performed aiming at identifying two structural changes or cracks, four parameters were being searched ( $x_{c1}$ ,  $x_{c2}$ ,  $a_1$  and  $a_2$ ), and the initial population was defined as 60. After selecting the initial population, the algorithm progresses with natural selection, mutation and crossover, and a new population is defined. Optimization is interrupted when the objective function  $S$  assumes a lower value than an established tolerance or when the maximum number of iterations is achieved. The tolerance was set to  $10^{-6}$ , because the variations on the crack parameters when the objective function  $S$  is lower than this are negligible for identification purposes, i.e., the identified damage position starts to vary in the order of 0.01 mm and the damage depth varies in the order of  $10^{-4}$  mm. The maximum number of iterations is defined as 100 times the number of variables: 200 iterations for the single crack problem and 400 iterations for the double crack problem. The probability of crossover was set to 0.9, and the three best individuals were selected from one generation to another [12, 23, 50].

In order to solve the optimization problem, a programming routine using the language of the MATLAB software was developed. In one of the programming lines, the ANSYS software is activated, and it starts running in batch mode. The ANSYS software, at its turn, uses as input data a second routine previously prepared, allowing for the numerical-computational calculation of the natural frequencies of beams for different positions and depths of cracks; after being estimated, these parameters are exported to a text file which is read again by the MATLAB,

allowing the optimization to continue. All this process occurs automatically, proving to be an appropriate, efficient and powerful alternative for solving the inverse problem of identifying cracks.

### 3 Results and discussion

Table 1 presents the values of all five resonant frequencies obtained experimentally using the OMA of the intact beam and with the different evaluated damages, with the precision allowed by the three different frequency bands described in Sect. 2.1. From case 1–4, the beam has a cut characterized by different depths; and, in Case 5, the beam has two structural changes. Table 2 presents the resonant frequencies obtained from the numerically generated noisy data. This data was obtained for the intact beam and for beams subjected to different inserted cracks, with the precision allowed by the set resolution. Table 3 presents the experimental difference ED calculated as in Eq. (1), relating Cases 1–10 with the respective undamaged beam (experimental or numerical).

As expected, as the depth of the structural change or crack increases, more significant decreases on the values of resonant frequencies of the beams were observed. The optimization algorithm was run for all ten cases, according to the values in Table 3. The results—positions and depths of the cracks found, as well as the percentage error (in modulus) referring to the real cuts and cracks—are presented in Tables 4, 5, 6, 7, 8, 9, 10, 11, 12 and 13. It is worth pointing out that, sometimes, the solution of the optimization problem can lead to a crack localized in  $L - x_c$  instead of crack localized in  $x_c$ , because of the symmetry of the boundary conditions (both cracks cause the same

**Table 3** Percentage difference calculated for each case

| Case | Experimental difference (%) |                 |                 |                 |                 |
|------|-----------------------------|-----------------|-----------------|-----------------|-----------------|
|      | ED <sub>1</sub>             | ED <sub>2</sub> | ED <sub>3</sub> | ED <sub>4</sub> | ED <sub>5</sub> |
| 1    | 0.07436                     | 0.11920         | 0               | 0               | 0.08650         |
| 2    | 0.22305                     | 0.35757         | 0.12270         | 0               | 0.25952         |
| 3    | 0.74351                     | 1.31109         | 0.36810         | 0.01285         | 1.03806         |
| 4    | 6.09667                     | 8.82004         | 2.26995         | 1.15681         | 6.92042         |
| 5    | 6.46840                     | 9.89274         | 4.41718         | 2.82776         | 7.87197         |
| 6    | 0.07392                     | 0.02699         | 0.19439         | 0.21246         | 0.14999         |
| 7    | 0.36953                     | 0.62094         | 0.26381         | 0.02550         | 0.47883         |
| 8    | 1.69991                     | 0.32397         | 0.70814         | 0.90933         | 0.17884         |
| 9    | 5.32151                     | 2.40280         | 0.93029         | 4.07921         | 0.13846         |
| 10   | 2.43902                     | 1.91684         | 0.54152         | 2.93193         | 1.69032         |

**Table 4** Structural change identified for Case 1

| Real cut            | Identified crack | Error (%) |
|---------------------|------------------|-----------|
| Case 1: $a/h = 5\%$ |                  |           |
| $a = 1.1$ mm        | $a = 1.16$ mm    | 5.45      |
| $x_c = 22.0$ cm     | $x_c = 22.86$ cm | 3.91      |

**Table 5** Structural change identified for Case 2

| Real cut             | Identified crack | Error (%) |
|----------------------|------------------|-----------|
| Case 2: $a/h = 10\%$ |                  |           |
| $a = 2.2$ mm         | $a = 2.22$ mm    | 0.91      |
| $x_c = 22.0$ cm      | $x_c = 21.35$ cm | 2.96      |

**Table 6** Structural change identified for Case 3

| Real cut             | Identified crack | Error (%) |
|----------------------|------------------|-----------|
| Case 3: $a/h = 20\%$ |                  |           |
| $a = 4.5$ mm         | $a = 4.69$ mm    | 4.22      |
| $x_c = 22.0$ cm      | $x_c = 21.70$ cm | 1.36      |

**Table 7** Structural change identified for Case 4

| Real cut             | Identified crack | Error (%) |
|----------------------|------------------|-----------|
| Case 4: $a/h = 50\%$ |                  |           |
| $a = 11.1$ mm        | $a = 11.31$ mm   | 1.89      |
| $x_c = 22.0$ cm      | $x_c = 21.90$ cm | 0.46      |

**Table 8** Structural change identified for Case 5

| Real cut   | Identified crack | Error (%) |
|--|------------------|-----------|
| Case 5 (two cuts): $a/h = 50\%$ and $a/h = 25\%$ |                  |           |
| $a = 11.1$ mm                                    | $a = 10.96$ mm   | 1.26      |
| $x_c = 22.0$ cm                                  | $x_c = 21.97$ cm | 0.14      |
| $a = 5.6$ mm                                     | $a = 6.02$ mm    | 7.50      |
| $x_c = 59.0$ cm                                  | $x_c = 59.70$ cm | 1.17      |

**Table 9** Crack identified for Case 6

| Real crack          | Identified crack | Error (%) |
|---------------------|------------------|-----------|
| Case 6: $a/h = 8\%$ |                  |           |
| $a = 1.77$ mm       | $a = 1.71$ mm    | 3.39      |
| $x_c = 12.0$ cm     | $x_c = 11.42$ cm | 4.83      |

**Table 10** Crack identified for Case 7

| Real crack           | Identified crack | Error (%) |
|----------------------|------------------|-----------|
| Case 7: $a/h = 15\%$ |                  |           |
| $a = 3.32$ mm        | $a = 3.27$ mm    | 3.31      |
| $x_c = 50.8$ cm      | $x_c = 50.63$ cm | 0.33      |

**Table 11** Crack identified for Case 8

| Real crack           | Identified crack | Error (%) |
|----------------------|------------------|-----------|
| Case 8: $a/h = 23\%$ |                  |           |
| $a = 5.10$ mm        | $a = 5.27$ mm    | 3.33      |
| $x_c = 31.0$ cm      | $x_c = 30.96$ cm | 0.13      |

**Table 12** Crack identified for Case 9

| Real crack           | Identified crack | Error (%) |
|----------------------|------------------|-----------|
| Case 9: $a/h = 40\%$ |                  |           |
| $a = 8.86$ mm        | $a = 8.86$ mm    | 0.00      |
| $x_c = 43.20$ cm     | $x_c = 43.07$ cm | 0.30      |

**Table 13** Cracks identified for Case 10

| Real crack  | Identified crack | Error (%) |
|---|------------------|-----------|
| Case 10 (two cracks): $a/h = 30\%$ and $a/h = 18\%$ |                  |           |
| $a = 6.65$ mm                                       | $a = 6.58$ mm    | 1.05      |
| $x_c = 27.0$ cm                                     | $x_c = 27.09$ cm | 0.33      |
| $a = 3.99$ mm                                       | $a = 4.11$ mm    | 3.01      |
| $x_c = 63.0$ cm                                     | $x_c = 63.38$ cm | 0.60      |

changes on the beam's natural frequencies in a free-free beam).

Analyzing the results, one can observe that the proposed method is capable of identifying the parameters of a structural change or a crack with an acceptable accuracy

for many applications in engineering, allowing a maintenance intervention to be made before crack's depth reaches a pre-determined unacceptable value. The largest error reported was 7.50%, corresponding to 0.42 mm in the depth of cut 2, in the Case 5. In that case (identification of

double cracks), the control of a larger number of characteristic frequencies would probably lead to more accurate results, as discussed previously. In the present study, only two preliminary double crack cases were evaluated, providing encouraging results; further studies could test the efficiency of the presented method in identifying multiple cracks, especially with smaller depths.

When analyzing the results regarding the cracks generated numerically with noise (Cases 6–10), one observes that the method was able to identify these damages (even the smaller ones) with minor errors. This happens because, despite the added noise caused a significant variability in the inertance amplitude data (vertical axis of Fig. 3), there are relative small deviations on the peak frequencies values of the pure and noisy data (horizontal axis of Fig. 3), and these are the parameters computed for the algorithm to be run. In addition, it is interesting to notice that the first natural frequency value regarding the Case 6 was higher than the corresponding frequency of the undamaged beam, as in Table 2. This effect, which was obviously produced by the added noise, did not hinder the crack to be identified with an appropriate precision.

Another issue to be analyzed is the fact that, with the equipment used in the OMA, it would not be possible to identify cracks having depths smaller than 5% the height of the beam. This is so because the resolution of the data acquisition system does not allow detecting the variation between the resonant frequencies of the beam in intact condition and with a small cut. Such effect can be illustrated by analyzing the 3rd and 4th natural frequencies obtained in Case 1, as in Table 3. Although the structural change has produced reductions on those frequencies, they were too subtle to be captured by the measurement system used (even so, it was possible to identify that structural change with the reduction pattern obtained).

Therefore, one observes that the applicability of the proposed method to the identification of small depth cracks ( $a/h < 10\%$ ) becomes conditioned to the resolution of the hardware used. From a practical point of view, if it becomes necessary to identify cracks in even more incipient stages ( $a/h = 2\%$ , for example), it would be necessary to use a system that would allow this level of detail, i.e., a system that could carry out the acquisition of more points in the same frequency band. Actually, since at least one resonant frequency shift was not detected by the utilized equipment for Cases 1 and 2 (see Table 3), there are only indications that the proposed method is effective in detecting these damage depths. A way to ensure the efficacy would be the testing of damages of these magnitudes with better resolution equipment.

A limitation of the presented methodology is the fact that the number of damages was known in advance for the single crack cases, i.e., only one crack was parameterized

in the numerical model. Regarding the double damage cases, the algorithm ran with the possibility of one or two cracks to be present, since a crack could assume a virtual depth of  $a = 0$ , which represents the absence of the crack [see the lower bound values in Eqs. (14) and (15)]. Further studies could parameterize and test a model where several cracks could be present, considering their depths ranging from  $0 \leq a_n \leq 0.9h$ , which would be a way to try to solve the problem without previously knowing the number of present structural changes or cracks.

Finally, it is clear that, in real systems, there is no possibility of concluding with absolute certainty that differences observed in the resonant frequencies were caused by the appearance of cracks. Since these frequency shifts can be caused also by other factors—such as other types of faults and accommodations—, the assertiveness of the present method is conditioned to this fact, as all the other methods based on frequencies observation presented by the literature. In other words, if a crack is identified by the proposed methodology, a simple further investigation should be made in order to proof the existence of the damage, as a visual inspection.

## 4 Conclusions

Although the literature presents a wide range of possibilities for solving the inverse problem of identifying cracks in beams, there are difficulties in the process of implementation of these techniques by the industry. The present work has presented a method for carrying out such identification aiming at operational conditions, i.e., a method to identify small structural changes which could represent cracks remotely (with no need of technical inspection on the location of the structure for data acquiring) and in almost real time (depending only on the time consumed to solve the optimization problem), in beams subjected to unknown random loading, minimizing the measurement equipment used to a single accelerometer.

The proposed method combines an OMA based procedure, a parameterized numerical-computational model of the damaged beam, and an optimization problem solved by using genetic algorithms, in order to determine—by controlling the characteristic frequencies of the structure—the position and depth of the cracks. The technique was tested in a steel beam with square cross-section and on numerically generated noisy data. The results show that the method is capable of detecting single and double damages with an acceptable accuracy for many applications in structural engineering. A cut with a depth  $a/h = 5\%$  (Case 1) was identified. There were found no previous studies in the literature that were able to identify a crack of this magnitude—the smallest cracks earlier identified,

numerically or experimentally, had a depth of  $a/h = 10\%$ . Although the found results are encouraging, it is worth pointing out that they represent a preliminary assessment of the proposed methodology. Before being applied in real situations, the presented method should be tested for a wider range of cases, with the objective of testing its efficiency in statistical terms.

Based on the steps described in the present work, a hardware can be developed aiming at monitoring the integrity of beams in an automatized and on-line way. The smaller the cracks one wishes to identify are, the bigger the capacity to acquire data and higher the resolution of the hardware in frequency must be. Further works could analyze the use of the proposed method in beams with closed cracks, excited by their operational use in in situ applications.

**Acknowledgements** The authors thank the Human Resources Program 24 (PRH-24) of the National Petroleum Agency (ANP) of Brazil for granting the scholarship that allowed the development of the present work.

## References

- Montanari L, Spagnoli A, Basu B, Broderick B (2015) On the effect of spatial sampling in damage detection of cracked beams by continuous wavelet transform. *J Sound Vib* 345:233–249
- Dimarogonas AD (1996) Vibration of cracked structures: a state of art review. *Eng Fract Mech* 55:831–857
- Rizos PF, Aspragathos N, Dimarogonas AD (1990) Identification of crack location and magnitude in a cantilever beam from the vibration modes. *J Sound Vib* 138:381–388
- Nikolakopoulos PG, Katsareas DE, Papadopoulos CA (1997) Crack identification in frame structures. *Comput Struct* 64:389–406
- Fernández-Sáez J, Navarro C (2002) Fundamental frequency of cracked beams in bending vibrations: an analytical approach. *J Sound Vib* 256:17–31
- Lee J (2009) Identification of multiple cracks in a beam using natural frequencies. *J Sound Vib* 320:482–490
- Mazanoglu L, Sabuncu M (2012) A frequency based algorithm for identification of single and double cracked beams via a statistical approach used in experiment. *Mech Syst Signal Process* 30:168–185
- Gillich GR, Praisach ZI (2014) Modal identification and damage detection in beam-like structures using the power spectrum and time–frequency analysis. *Signal Process* 96:29–44
- Moezi SA, Zakeri E, Zare A, Nedaei M (2015) On the application of modified cuckoo optimization algorithm to the crack detection problem of cantilever Euler–Bernoulli beam. *Comput Struct* 157:42–50
- Fernández-Sáez J, Morassi A, Pressacco M, Rubio L (2016) Unique determination of a single crack in a uniform simply supported beam in bending vibration. *J Sound Vib* 371:94–109
- Mungla MJ, Sharma DS, Trivedi RR (2016) Identification of a crack in clamped-clamped beam using frequency-based method and genetic algorithm. *Proced Eng* 144:1426–1434 (**12th international conference on vibration problems**)
- Eroglu U, Tufecki E (2016) Exact solution based finite element formulation of cracked beams for crack detection International. *J Solids Struct* 96:240–253
- Zhang K, Yan X (2017) Multi-cracks identification method for cantilever beam structure with variable cross-sections based on measured natural frequency changes. *J Sound Vib* 387:53–65
- Owolabi GM, Swamidas ASJ, Seshadri R (2003) Crack detection in beams using changes in frequencies and amplitudes of frequency response functions. *J Sound Vib* 265:1–22
- Greco A, Pau A (2012) Damage identification in Euler frames. *Comput Struct* 92–93:328–336
- Douka E, Loutridis S, Trochidis A (2003) Crack identification in beams using wavelet analysis. *Int J Solids Struct* 40:3557–3569
- Hadjileontiadis LJ, Douka E, Trochidis A (2005) Fractal dimension analysis for crack identification in beam structures. *Mech Syst Signal Process* 19:659–674
- Lu XB, Liu JK, Lu ZR (2013) A two-step approach for crack identification in beam. *J Sound Vib* 332:282–293
- Khiem NT, Tran HT (2014) A procedure for multiple crack identification in beam-like structures from natural vibration mode. *J Vib Control* 20:1417–1427
- Xu YF, Zhu WD, Liu J, Shao YM (2014) Identification of embedded horizontal cracks in beams using measured mode shapes. *J Sound Vib* 333:6273–6294
- Srinivasarao D, Rao KM, Raju GV (2010) Crack identification on a beam by vibration measurement and wavelet analysis. *Int J Eng Sci Technol* 2:907–912
- Attar M (2012) A transfer matrix method for free vibration analysis and crack identification of stepped beams with multiple edge cracks and different boundary conditions International. *J Mech Sci* 57:19–33
- Khaji N, Mehrjoo M (2014) Crack detection in a beam with an arbitrary number of transverse cracks using genetic algorithms. *J Mech Sci Technol* 28:823–836
- Hakim SJS, Abdul Razak H, Ravanfar SA (2015) Fault diagnosis on beam-like structures using artificial neural networks. *Measurement* 76:45–61
- Altunisik AC, Okur FY, Kahya V (2017) Modal parameter identification and vibration based damage detection of a multiple cracked cantilever beam. *Eng Fail Anal* 79:154–170
- Saeed RA, Galybin AN, Popov V (2012) Crack identification in curvilinear beams by using ANN and ANFIS based on natural frequencies and frequency response functions. *Neural Comput Appl* 21:1629–1645
- Fernández-Sáez J, Rubio L, Navarro C (1999) Approximate calculation of the fundamental frequency for bending vibrations of cracked beams. *J Sound Vib* 225:345–352
- Loya JA, Rubio L, Fernández-Sáez J (2006) Natural frequencies for bending vibrations of Timoshenko cracked beams. *J Sound Vib* 290:640–653
- Hou C, Lu Y (2016) Identification of cracks in thick beams with a cracked beam element model. *J Sound Vib* 385:104–124
- Chouiyakh H, Azrar L, Alnefaie K, Akourri O (2017) Vibration and multi-crack identification of Timoshenko beams under moving mass using the differential quadrature method. *Int J Mech Sci* 120:1–11
- Law SS, Lu ZR (2005) Crack identification in beam from dynamic responses. *J Sound Vib* 285:967–987
- Andreas U, Baragatti P (2011) Cracked beam identification by numerically analyzing the nonlinear behaviour of the harmonically forced response. *J Sound Vib* 330:721–742
- Neves AC, Simões FMF, Pinto da Costa A (2016) Vibrations of cracked beams: discrete mass and stiffness models. *Comput Struct* 168:68–77

34. Bovsunovsky A, Surace C (2015) Non-linearities in the vibrations of elastic structures with a closing crack: a state of the art review. *Mech Syst Signal Process* 62–63:129–148
35. Ewins DJ (2000) *Modal testing: theory, practice and application*. Research Studies Press LTD, Baldock
36. Gomes HM, Almeida FJF (2014) An analytical dynamic model for single-cracked beams including bending, axial stiffness, rotational inertia, shear deformation and coupling effects. *Appl Math Model* 38:938–948
37. Yamuna P, Sambasivarao K (2014) Vibration analysis of beam with varying crack location. *Int J Eng Res General Sci* 2:1008–1017
38. Oliveira Filho MVM, Ipiña JEP, Bavastri CA (2017) Analysis of sensor placement in beams for crack identification. In: *MecSol—proceedings of the 6th international symposium on solid mechanics*, pp 536–553
39. Lee J (2009) Identification of multiple cracks in a beam using vibration amplitudes. *J Sound Vib* 326:205–212
40. Hou C, Lu Y (2017) Experimental study of crack identification in thick beams with a cracked beam element model. *J Eng Mech* 143(6). [https://doi.org/10.1061/\(ASCE\)EM.1943-7889.0001215](https://doi.org/10.1061/(ASCE)EM.1943-7889.0001215)
41. Cao M, Xu W, Ostachowicz W, Su Z (2014) Damage identification for beams in noisy conditions based on Teager energy operator-wavelet transform modal curvature. *J Sound Vib* 333:1543–1553
42. Cao M, Radzienski M, Xu W, Ostachowicz W (2014) Identification of multiple damage in beams based on robust curvature mode shapes. *Mech Syst Signal Process* 46:468–480
43. He S, Ng C (2017) Guided wave-based identification of multiple cracks in beams using a Bayesian approach. *Mech Syst Signal Process* 84:324–345
44. Khavita S, Joseph Daniel R, Sumangala K (2016) High performance MEMS accelerometers for concrete SHM applications and comparison with COTS accelerometers. *Mech Syst Signal Process* 66–67:410–424
45. Ebrahimkhanlou A, Salamone S (2017) Acoustic emission source localization in thin metallic plates: a single-sensor approach based on multimodal edge reflections. *Ultrasonics* 78:134–145
46. Kanaparthi S, Sekhar VR, Badhulika S (2016) Flexible, eco-friendly and highly sensitive paper antenna based electromechanical sensor for wireless human motion detection and structural health monitoring. *Extreme Mech Lett* 9:324–330
47. Xiang J, Chen X, Mo Q, He Z (2007) Identification of crack in a rotor system based on wavelet finite element method. *Finite Elem Anal Des* 43:1068–1081
48. Orhan S, Lüy M, Dirikolu MH, Zorlu GM (2016) The effect of crack geometry on the non-destructive fault detection in a composite beam. *International. J Acoust Vib* 21:271–273
49. Meirovitch L (1986) *Elements of vibration analysis*. Virginia Polytechnic Institute State University, Mc Graw Hill, 2nd Edn
50. Mehrjoo M, Khaji N, Ghafory-Ashtiany M (2014) New timoshenko-cracked beam element and crack detection in beam-like structures using genetic algorithm. *Inverse Prob Sci Eng* 22:359–382